Audio Engineering Society
Convention Paper

Presented at the 115th Convention
2003 October 10–13 New York, New York

Practical Implementation of Constant Beamwidth Transducer (CBT) Loudspeaker Circular-Arc Line Arrays

D. B. (Don) Keele, Jr., *AES Fellow*

Harman/Becker Automotive Systems
Martinsville, IN 46151, USA
E-mail: DKeele@Harman.com

ABSTRACT

To maintain constant beamwidth behavior, CBT circular-arc loudspeaker line arrays require that the individual transducer drive levels be set according to a continuous Legendre shading function. This shading gradually tapers the drive levels from maximum at the center of the array to zero at the outside edges of the array. This paper considers approximations to the Legendre shading that both discretize the levels and truncate the extent of the shading so that practical CBT arrays can be implemented. It was determined by simulation that a 3-dB stepped approximation to the shading maintained out to –12 dB did not significantly alter the excellent vertical pattern control of the CBT line array. Very encouraging experimental measurements were exhibited by a pair of passively-shaded prototype CBT arrays using miniature wide-band transducers.

0. INTRODUCTION

Constant beamwidth transducer (CBT) array theory is based on un-classified military under-water transducer research done in the late 1970s and early 80s [1, 2]. The research describes a curved-surface transducer in the form of a spherical cap with frequency-independent Legendre shading that provides wide-band extremely-constant beamwidth and directivity behavior with virtually no side lobes. The theory was applied to loudspeaker arrays by Keele in 2000 [3] where he extended the concept to arrays based on toroid-shaped curved surfaces and to circular-arc line arrays. Keele also extended the concept to straight-line and flat-panel CBT arrays with the use of signal delays [4]. In [5], Keele further analyzed the full-sphere sound field of CBT loudspeaker line arrays. Appendix 1 contains a brief review of CBT theory.

CBT arrays require Legendre function shading of the transducer drive levels in order to maintain the unique frequency-invariant pattern control of the CBT arrays. CBT theory dictates that each transducer in the array be driven with different levels that follow the continuous Legendre shading function. The Legendre shading gradually tapers the drive levels of each transducer from maximum at the center of the array to zero at the outside edges of the array. This paper considers the practical implementation aspects of CBT circular-arc line arrays and specifically to methods required to apply the Legendre shading to the drive levels of the individual transducers that make up the array.

Shading methods investigated included the question of whether banks of transducers can be assigned the same drive level according to a stepped approximation to the Legendre shading function and whether the shading can be truncated after dropping below a certain minimum level. A series of simulations were run with different step values and different truncations to evaluate what level of approximation was acceptable. It was determined that a 3-dB stepped approximation to the shading maintained out to –12 dB did not appreciably alter the pattern control properties of the CBT array.

The stepped gain changes can be done passively with simple resistor networks, auto transformers, driver impedance changes, series-parallel connection combinations, or actively by changing the gain of individual amplifiers driving each speaker or groups of speakers.

The effect of stepped and truncated shading on the electrical power loss and sound pressure level (SPL) loss of the CBT array was also investigated.

A pair of prototype CBT line arrays were constructed using miniature wide-band transducers. Each was designed to use two different driver sizes: small and large. Both arrays were designed to provide the same vertical coverage and the same beamwidth low-frequency control limit.

Two arrays were constructed with different size drivers to test the high-frequency beamwidth control of the arrays. These two arrays were intended to answer the question of whether very-small drivers spaced very-close together are (in fact) required to operate up to 16 kHz, or could larger drivers be used with their inherent high-frequency beaming to control beamwidth up to 16 kHz. Both arrays were passively shaded using a combination of parallel-series connections, resistor L-pad attenuators, and auto transformers.

Both arrays were measured using a full-sphere automated polar test system with very encouraging results. Results indicate that operation to 16 kHz does indeed require the use of very-small closely-spaced wideband drivers. The reduced low-frequency capability of these very-small drivers means that at least a two-way design using a combination of small and large drivers is required to operate wideband from 100 Hz to 16 kHz.

This paper is organized as follows. Sections 1 and 2 describe stepped and truncated approximations to the Legendre shading required by the CBT curved-line arrays. Section 3 describes the 3-dB stepped and minus-12-dB truncated shading chosen for implementing the CBT prototype arrays and also displays a series of simulated performance results for an example array using the chosen shading. Section 4 describes the relationship between the array wedge angle and the resultant vertical beamwidth angle, while section 5 describes the shading power loss and SPL attenuation due to the various shadings. Section 6 describes several methods to implement the stepped shading. Two experimental CBT prototype arrays are described in Section 7, while Section 8 describes the results of experimental measurements on the prototypes. Section 9 concludes and section 10 lists the references. The appendices in Sections 11 – 13 present a review of CBT theory, describe the numerical simulator used to predict the array's coverage patterns, and contains two tables that show simulated performance results for stepped shading and truncated shading approximations.

1. STEPPED LEGENDRE SHADING

This section investigates the effects of approximating the continuous Legendre CBT shading with discrete steps. A stepped approximation to the shading is desirable because groups of transducers can then be assigned the same drive level which simplifies application of the shading.

Figure 1 illustrates an example of continuous Legendre shading (Eq. (3) Appendix 1.) along with a 6-dB-stepped approximation to the shading. The shading is maximum (no attenuation) in the center of the array and falls to zero (high attenuation) at the outside edges of the array.

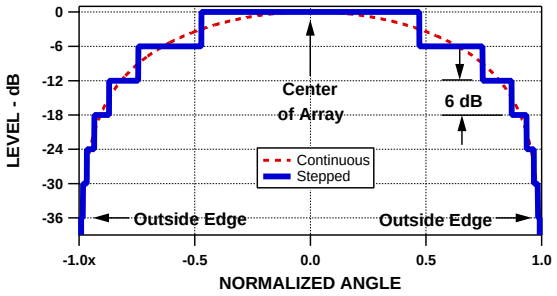

Fig. 1. Continuous (dashed line) and 6-dB-stepped approximate Legendre (solid line) shading for CBT curved-line arrays. The shading is plotted on a log vertical scale in dB versus normalized wedge angle with 0.0 being the center of the array and ±1 being the outside edges.

The results of several simulations for varying step sizes are shown in Appendix 3 Table 1, which was generated using the simulator described in Appendix 2. In this table, step sizes of 0 dB (continuous shading), 3 dB, 6 dB, 9 dB, and single step (no shading) were simulated. The 3-dB step size appears to offer the best combination of attributes that least compromises the performance as compared to continuous shading.

2. TRUNCATION OF LEGENDRE SHADING

This section investigates the effects of truncating the continuous Legendre CBT shading at points where the level drops below a certain minimum. Truncating the shading is desirable because it eliminates transducers on the outside edges of the array that are greatly attenuated and may not be contributing effectively to the performance of the array.

Figure 2 shows an example of continuous Legendre shading (dashed line) along with minus-12-dB truncated shading (solid line).

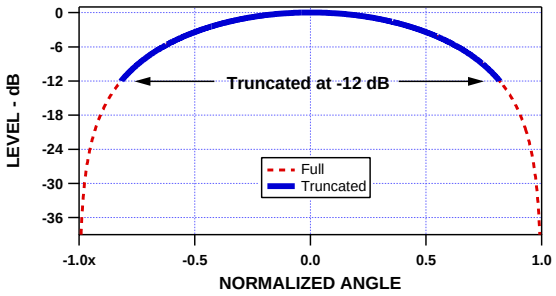

Fig. 2. Continuous and minus-12-dB truncated Legendre shading for CBT curved-line arrays.

The results of several simulations varying truncation levels are shown in Appendix 3 Table 2, which was generated using the simulator described in Appendix 2. In this table, truncation levels of –18, -15, -12, -9, and -6 dB were investigated. The minus-12-dB truncation level appears to offer the best combination of attributes that least compromises the performance as compared to continuous shading.

3. STEPPED and TRUNCATED LEGENDRE SHADING

This section investigates combining the stepped and truncated shading approximations to optimize implementation of the shading.

3.1. 3-dB Steps and Truncated at –12 dB

Figure 3 illustrates 3-dB steps combined with minus-12-dB truncation (solid line). As before, continuous shading is also shown in the graph (dashed line). Note that the continuous shading is down 6 dB at a normalized angle of about 0.64. This means that the array's beamwidth is about 64% of the wedge angle of the array if implemented with either shading.

3.1.1. Shading

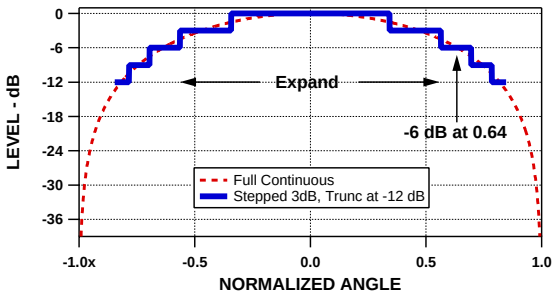

Fig. 3. Continuous and 3-dB stepped and minus-12-dB truncated approximate Legendre shading for CBT curved-line arrays.

3.1.2. Expanded Shading

Now that the outside portions of the stepped shading have been truncated, effectively eliminating any drivers on the outside of the array because they have been turned off, the remaining central portion of the shading can be expanded to fill the complete wedge angle of the array. This is shown in Fig. 4. Note that the outside edges of the array are attenuated by only 12 dB and that five discrete steps of 0, -3, -6, -9, and –12 dB have been created. Note furthermore that the shading is now down 6 dB at a normalized angle of about 0.75. This now means that the array's beamwidth widens to about 75% of the wedge angle of the array due to the truncated and expanded shading.

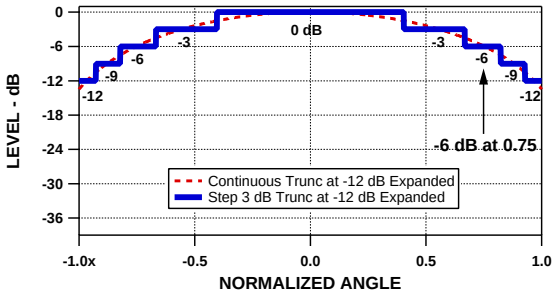

Fig. 4. Expanded continuous and 3-dB stepped and minus-12-dB truncated approximate Legendre shading for CBT curved-line arrays. Note that this shading is the expanded version of the shading of Fig. 3. The resultant stepped shading has five discrete steps of 0, -3, -6, -9, and –12 dB. Note that the 0-dB step is centrally located and is contained on one step. The remaining steps are divided in two equal parts each of which are on opposite ends of the array.

3.1.3. Proportion of Drivers at Each Level

The five discrete shade steps shown in Fig. 4 contain the following proportions of the array's total wedge angle. These proportions roughly reflect the percentages of the total drivers at each level assuming a large number of small drivers.

The following is a list of the percentages of the total drivers at each level (or bank) for the 3-dB-stepped and minus-12-dB truncated shading:

Bank 1 (0 dB):	40.4%
Bank 2 (-3 dB):	26.2%
Bank 3 (-6 dB):	15.5%
Bank 4 (-9 dB):	10.5%
Bank 5 (-12 dB):	7.4%
Total	100%

These percentages show that approximately two thirds of the total number of drivers are contained in the top two banks, 0 dB and -3 dB (40.4 + 26.2 = 66.6%). The remaining third of the drivers are attenuated by at least 6 dB.

3.2. Simulated Performance Results

The following shows simulated performance results for the 3-dB-stepped and minus-12-dB truncated shading. These simulations were run using the simulator described in Appendix 2. A one-meter-high 62.5°-wedge-angle CBT curved-line array was simulated.

3.2.1. Simulated Curved-Line CBT Array

A 1-m-high 62.5°-wedge-angle array was chosen to illustrate the performance results of the 3-dB-stepped and minus-12-dB truncated shading. This array should provide a theoretical vertical beamwidth of 47° (= 0.75 x 62.5°). (Note: If this array were shaded with a non-truncated Legendre shading, it would have a beamwidth of 40° (= 0.64 x 62.5°).) The array contains 201 point sources spaced at approximately 5.3 mm (0.21") apart, which insures operation to above 20 kHz before grating lobes occur.

The side, front, and top views of the simulated array are shown in Fig. 5. In these views, the dot size of the point sources are varied to reflect the shading strength.

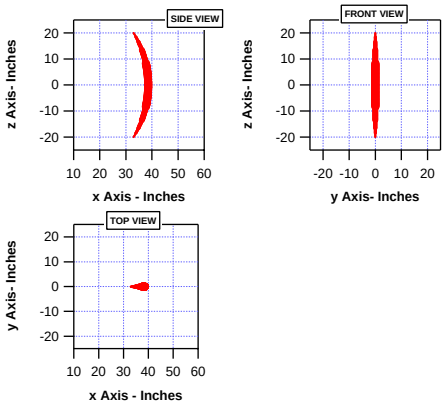

Fig. 5. Shape of 62.5°-wedge-angle 1m-high CBT curved-line array used to simulate the performance of a 3-dB-stepped and minus-12-dB truncated Legendre shaded array. Side view (upper left), front view (upper right, and top view (lower left). The array contains 201 point sources spaced at 5.3 mm (0.21") which insures operation to above 20 kHz. Shading follows the stepped and truncated function of Fig. 4.

3.2.2. Beamwidth vs. Frequency

The array's predicted beamwidth versus frequency is shown in Fig. 6. Note the roughly uniform 50° beamwidth at 800 Hz and above.

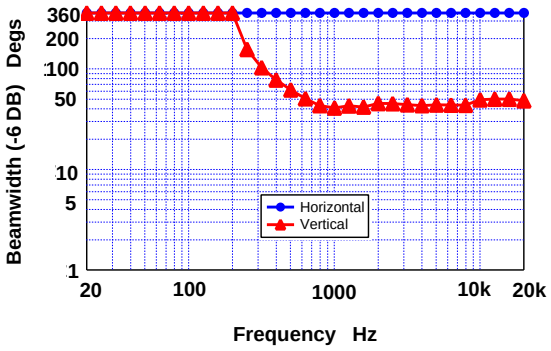

Fig. 6. Simulated beamwidth vs. frequency for the array of Fig. 5.

3.2.3. Directivity vs. Frequency

The directivity index and Q of the array are shown in Fig. 7. Note the uniform directivity of about 4 to 5 dB at 630 Hz and above.

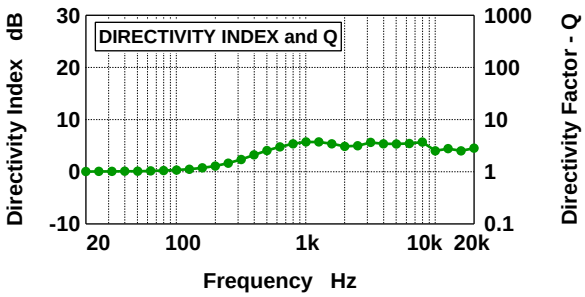

Fig. 7. Simulated directivity factor and index vs. frequency for the array of Fig. 5.

3.2.4. On-Axis Loss vs. Frequency

The array's simulated on-axis loss is shown in Fig. 8. This plot indicates how much on-axis attenuation the array imposes due to its curvature as compared to the situation where all the sources add in phase at the observation point. The array exhibits the typical 3-dB/octave or 10-dB/decade CBT rolloff that is exhibited by all CBT line arrays throughout their operating range [3] .

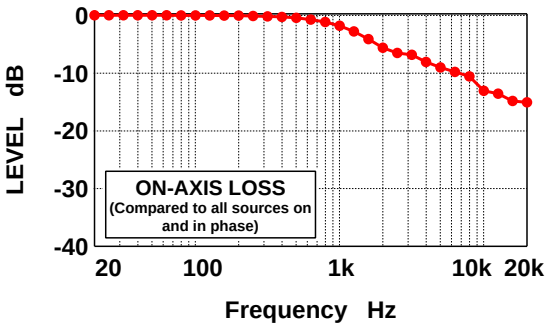

Fig. 8. . Simulated on-axis loss vs. frequency for the array of Fig. 5.

3.2.5. Vertical Polars

Figure 9 shows the predicted vertical polars of the array at all one-third-octave centers from 630 Hz to 20 kHz. The polar curves have not been on-axis normalized. This means that the level on axis (points at 0° to the right) rises or falls depending on the on-axis loss (Fig. 8). Note the extreme uniformity of the polars.

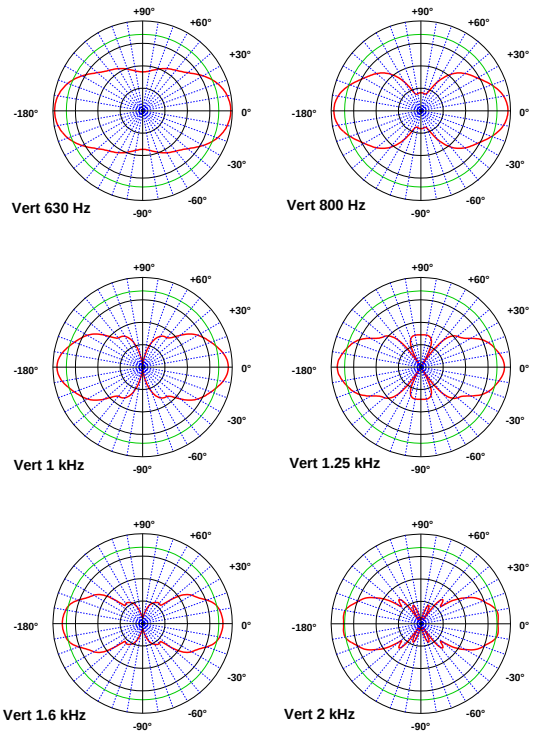

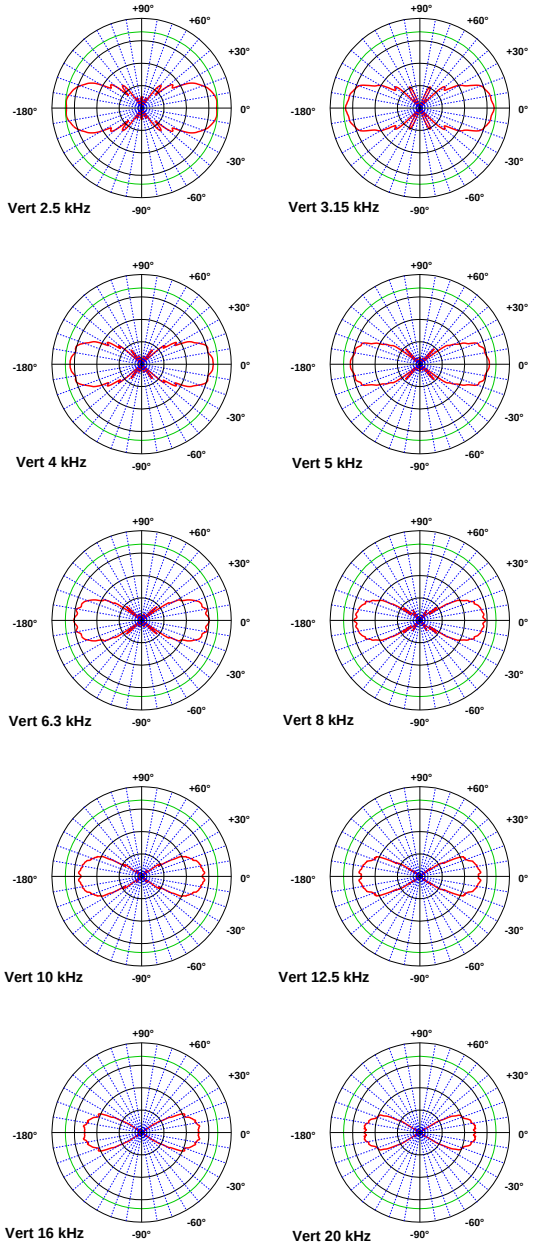

Fig. 9. Simulated vertical polars for the array of Fig. 5. The polars are simulated at one-third-octave intervals from 630 Hz to 20 kHz (top to bottom and left to right). On axis faces to the right. Radiation is bi-directional because the array is composed of point sources which radiated equally well to the front and rear.

3.2.6. Foot Prints

Figure 10 shows selected axial foot prints of the array at octave intervals from 630 Hz to 10 kHz. Again note the extreme uniformity with frequency.

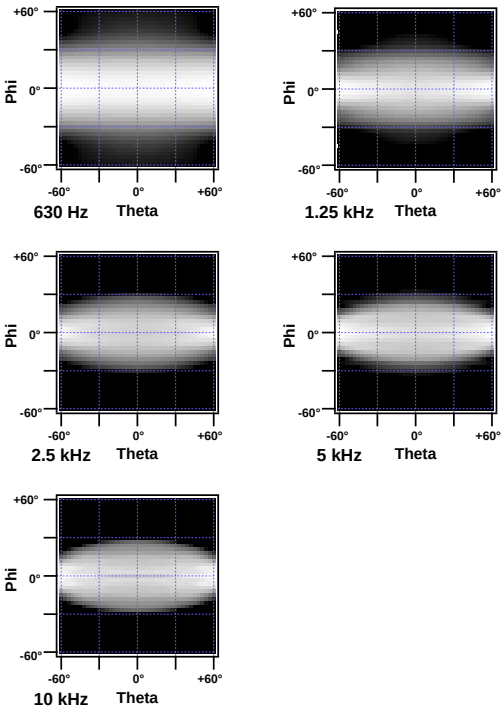

Fig. 10. Simulated axial foot prints for the array of Fig. 5. The foot prints are simulated at octave intervals from 630 Hz to 10 kHz (top to bottom and left to right). The foot print displays the normalized SPL in a rectangular ±60° region of on axis. The SPL is displayed in a 20-dB gray scale with white = 0 dB and black = -20 dB. Note uniformity.

4. RELATIONSHIP BETWEEN ARRAY WEDGE ANGLE AND VERTICAL BEAMWIDTH

As noted in passing earlier, truncating the Legendre shading changes the relationship between the array's circular wedge angle and its resultant vertical coverage angle. The beamwidth provided by the CBT array with full continuous non-truncated shading is 64% of the wedge angle [3], i.e., Beamwidth = 0.64 x WedgeAngle. The 3-dB stepped and 12-dB truncated shaded CBT array provides a wider beamwidth of 75% of the wedge angle, i.e., Beamwidth = 0.75 x WedgeAngle.

5. SHADING POWER LOSS and SPL REDUCTION

There are two separate broad-band shading losses to consider. First, the shading reduces the effective electrical power rating of the array because some of the drivers that make up the array are attenuated to implement the shading. Second, shading also reduces the SPL generated by the array for the same reason. Note that in the second case, this loss is broadband

and does not included the high-frequency rolloff due to the curvature of the array.

The electrical power loss due to shading of the CBT array can be compared to an equivalent array with all drivers operating with no attenuation. The SPL shading loss generated by the CBT array can also be compared to the axial SPL generated by a straight-line array with all units operating at equal levels and in phase.

As compared to the continuous and non-truncated Legendre shading, the stepped and truncated shading minimizes the power loss due to the shading because the outside drivers of the array are attenuated less than the full un-truncated shading.

The following two sections compare the shading power loss and SPL loss for various shading functions. The loss numbers were calculated by either integrating the shading function itself to get the SPL loss or by integrating the square of the shading function to get the power loss. Both integrations were done with respect to wedge angle.

The tables compare three different shadings:

1) 3-dB-stepped and minus-12-dB-truncated approximation to the Legendre shading (used in the following prototype),
2) continuous full Legendre shading (which essentially turns the farthest-most outside drivers off), and
3) Hann (cosine squared, a typical window used in signal processing included here for comparison only) shading.

5.1. Shading Electrical Power loss:

Hann:	-4.3 dB
Legendre, Full Continuous:	-3.2 dB
Legendre, 3-dB-Stepped and Truncated at –12 dB:	-2.3 dB

5.2. Shading SPL Loss:

Hann:	-6.0 dB
Legendre, Full Continuous:	-4.2 dB
Legendre, 3-dB-Stepped and Truncated at –12 dB:	-2.8 dB

5.3. General Shading Loss Comments

As compared to the continuous Legendre and Hann shadings, the stepped and truncated shading has the least loss of all, roughly 3 dB on-axis SPL loss and 2 dB power loss.

6. IMPLEMENTATION OF STEPPED SHADING

The stepped shading can be implemented passively with simple resistor networks, auto transformers, driver impedance changes, series-parallel connection combinations, or actively by changing the gain of individual amplifiers driving each speaker or groups of speakers.

7. EXPERIMENTAL PROTOTYPES

A pair of passively-shaded prototype CBT line arrays were constructed using miniature wide-band transducers. Both were designed to provide a 45º vertical beamwidth (-6 dB) with a 60º wedge angle and both were one-meter tall. Both were intended to control vertical beamwidth down to 670 Hz. Both used passive shading following the 3-dB-stepped and minus-12-dB-truncated approximation to the Legendre shading described in Section 3.

The first array uses 18-each 57mm (2.25”) full-range (80 Hz to 20 kHz) drivers spaced at 59 mm (2.32”) center to center. The second array uses 50-each 18.3mm (0.72”) limited-range (400 Hz to 20 kHz) drivers spaced at 21.2 mm (0.835”). The former driver is used in the Apple iMac, while the latter is used in several brands of laptop computers including Dell and Toshiba.

Two arrays were constructed to determine whether very-small drivers spaced very-close together are (in fact) required to operate up to 16 kHz, or could larger drivers be used with their inherent high-frequency beaming to operate up to 16 kHz. Both arrays were passively shaded using a combination of parallel-series connections and resistor L-pad attenuators.

7.1. Driver Selection

The drivers used in the prototype arrays are described in the following two sections.

7.1.1. Large Driver

The large driver (only large by comparison to the smaller miniature driver!) is a wide-band 57 mm (2.25”) unit used in the base of a popular all-in-one desktop home computer and is manufactured by Harman Multimedia. It utilizes a 34.3 mm (1.35”) diameter inverted aluminum dome with rubber surround and operates over the range of 80 Hz to 20 kHz with a power rating of 8 Watts. Fig. 11 shows front and rear views of this driver along side a ruler for size reference.

Fig. 11. Photo of the 57 mm (2.25") driver used in the large-driver CBT array. The ruler is a 15 cm (6") long.

7.1.2. Small Driver

The small driver is a wide-band 17.8 mm (0.7") miniature unit use in several brands of laptop computers and is manufactured by Harman Multimedia. It utilizes a 12.7 mm (0.5") diameter inverted aluminum dome with foam surround (and no spider!) and operates over the range of 400 Hz to 20 kHz with a power rating of 1.5 Watts. Fig. 12 shows top and bottom views of this driver along side a ruler for size reference.

Fig. 12. Photo of the 17.8 mm (0.7") diameter driver used in the small-driver prototype CBT array. . The ruler is a 15 cm (6") long.

7.2. Large-Driver Array Photos

The following two figures (Figs. 13 and 14) display photos of the large-driver array. The first shows an oblique side shot of the array and the second a front view of the array with the author's hand pointing to one of the drivers.

Fig. 13. Photo of the large-driver 60°-wedge-angle 1-m-high prototype array. The array uses 18 each 57mm (2.25") wide-band miniature transducers spaced at 59 mm (2.32") center to center.

Fig. 14. Close up of the front of the large-driver array of Fig. 13 with the author's hand pointing to one of the drivers. Wiring of the array was in progress.

7.3. Small-Driver Array Photos

Figures 15 and 16 display photos of the small-driver array. The first shows an oblique side shot of the array and the second a front view of the array with the author's hand pointing to one of the drivers.

Fig. 15. Photo of the small-driver 60°-wedge-angle 1-m-high prototype array. The array uses 50 each 17.8 mm (0.7") wide-band miniature transducers spaced at 21.2 mm (0.835") center to center. Wiring had not been completed at the time of the photo.

Fig. 16. Close up of the front of the small-driver array of Fig. 15 with the author's hand pointing to one of the drivers. Wiring of the array was in progress.

7.4. Side Views of the Arrays

Figures 17 and 18 display photos of the two arrays side by side. The first shows them on their backs with some distance separating them. The second shows them attached side by side in a vertically-oriented listening configuration with the author standing at the side.

Fig. 17. Oblique side views of the large-driver and small-driver arrays. Wiring is in progress.

Fig. 18. Prototype arrays attached side-by-side in listening configuration with author. Wiring for large-

driver array is composed of point-to-point wiring using barrier terminal strips mounted on the side of the array. The systems were crossed over at 800 Hz for listening.

7.5. Shading Implementation (Schematics)

The shading of the prototype arrays was implemented passively using series-parallel connections and resistor L-pad attenuators. The schematics for both arrays are described in the following two sections. The required 3-dB attenuation between the top two banks (Bank 1: 0 dB and Bank 2: -3 dB) was accomplished with only series-parallel connections.

7.5.1. Large-Driver Array

Figure 19 shows the schematic of the large-driver array which uses 18 drivers. The drivers are organized into five banks with the following quantities in each bank: 6, 6, 2, 2, and 2 (Bank 1: 0 dB, Bank 2: -3 dB, Bank 3: -6 dB, Bank 4: -9 dB, and Bank 5: -12 dB).

Bank 1 is composed of a series-parallel connection of six drivers in a 2 x 3 connection matrix with a an input voltage division ratio of 1/2 or -6 dB. Bank 2 also comprises six drivers in a series-parallel connection, but in a 3 x 2 matrix providing a 1/3 or -9.5 dB voltage division ratio. These two banks thus provide an approximate 3 dB attenuation ratio between the two (actually 3.5 dB). The remaining drivers are organized into three parallel sets of two driven by resistor L-pads to form the remaining banks.

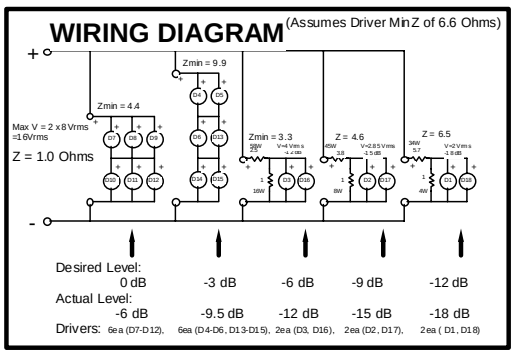

Fig. 19. Wiring diagram for the large-driver array. Shading is implemented passively with series-parallel wiring and resistor L-pad attenuation networks.

7.5.2. Small-Driver Array

Figure 20 shows the schematic of the small-driver array which uses 50 drivers. The drivers are organized into five banks with the following quantities in each bank: 18, 16, 8, 4, and 4 (Bank 1: 0 dB, Bank 2: -3 dB, Bank 3: -6 dB, Bank 4: -9 dB, and Bank 5: -12 dB).

Bank 1 is composed of a series-parallel connection of 18 drivers in a 3 x 6 connection matrix with an input voltage division ratio of 1/3 or -9.5 dB. Bank 2 comprises 16 drivers in a series-parallel connection, but in a 4 x 4 matrix providing a 1/4 or -12 dB voltage division ratio. These two banks thus provide an approximate 3 dB attenuation ratio between the two (actually 2.5 dB). The remaining drivers are organized into three series-parallel sets comprised of a 4 x 2, 2 x 2, and 2 x 2 matrices, each combination driven by resistor L-pads to form banks 3 to 5.

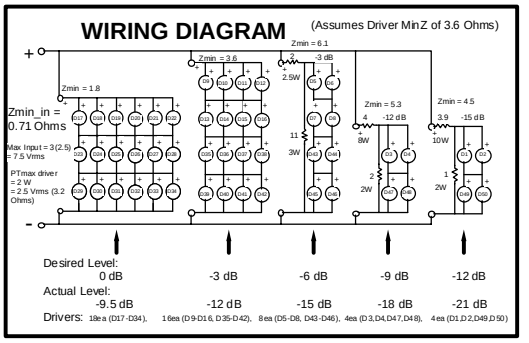

Fig. 20 Wiring diagram for the small-driver array. Shading is implemented passively with series-parallel wiring and resistor L-pad attenuation networks.

7.5.3. Low Input Impedance

As implemented, both networks exhibited an extremely low input impedance of about one ohm. To raise the input impedance, toriodal-wound auto-transformers were used to raise the input impedance from one ohm to four ohms (using a two to one step-down winding ratio).

8. PROTOTYPE MEASUREMENTS

This section displays several sets of measurement results on the two prototype CBT curved-line arrays. Both arrays were measured using JBL Pro's full-sphere automated polar test system at 6m, with rotation about the center of curvature of each array. Measurements included beamwidth, directivity, vertical polars, and 3D full-sphere polar balloon plots.

8.1. Polar Measurement Setup

Figure 21 shows a depiction of the polar measurement setup showing the location of the array, the test microphone, and the center of rotation. Both

arrays were rotated about their centers of curvature which was 1 m behind the front of the array. Most measurements were taken with the test microphone located at a distance of 6 m from the center of rotation (5 meters from the front of the array). Data was gathered at 5° increments at every one-third-octave center frequency from 125 Hz to 16 kHz.

An additional set of polars (not shown) were taken at a distance of 1.5 m from the center of rotation (only 0.5 m from the front of the array). The close-in polar measurements essentially duplicated the results at 6 m. This essentially verifies that the CBT array's radiation pattern is independent of distance as noted in Appendix 1.

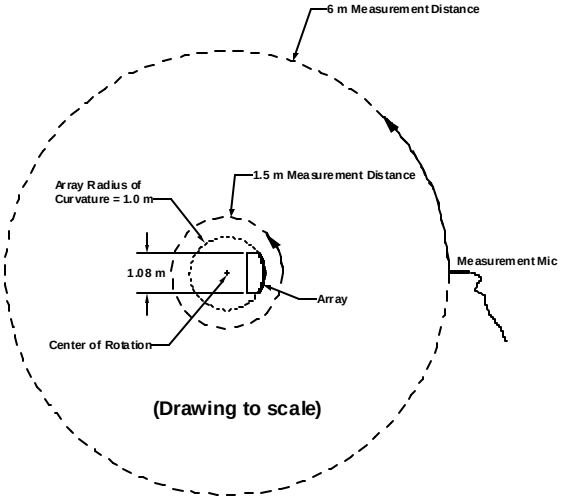

Fig. 21. Illustration of the polar measurement setup for the prototype arrays. The array was rotated around its center of curvature with the test mic located 6 m away from the center of rotation. An additional set of data was gathered near the array with the mic located only 1.5 m away from the center of rotation (0.5 m away from the front of the away).

8.2. Beamwidth vs. Frequency

This section shows the measured vertical and horizontal beamwidth (-6 dB) versus frequency of both arrays over the range of 125 Hz to 16 kHz.

8.2.1. Large-Driver Array

Figure 22 shows the beamwidth of the large-driver prototype array. Vertical beamwidth is well maintained at about 45° from 800 Hz to 5 kHz. Above 5 kHz the beamwidth widens suddenly because the drivers are spaced to far apart with respect to wavelength in this frequency range. At 6.3 kHz and above, both the horizontal and vertical beamwidth narrows because of the inherent narrowing coverage of the driver used in the array.

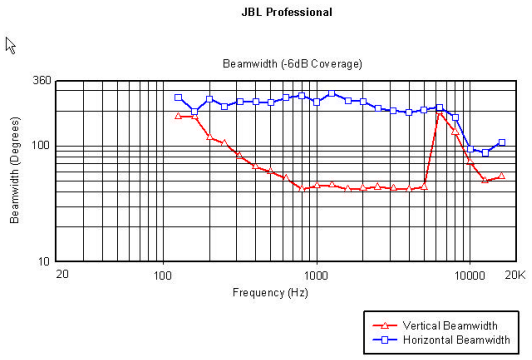

Fig. 22. Measured beamwidth vs. frequency of the large-driver prototype array of Fig. 13.

8.2.2. Small-Driver Array

Figure 23 shows the beamwidth of the small-driver prototype array. Both vertical and horizontal beamwidth plots are very well behaved. Vertical beamwidth is maintained at about 46º (±4º) from 800 Hz and above. Horizontally, the coverage is 180° or more over the whole operating range.

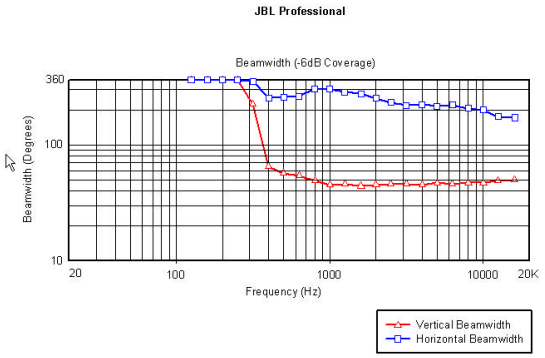

Fig. 23. Measured beamwidth vs. frequency of the small-driver prototype array of Fig. 15.

8.3. Directivity vs. Frequency

This section illustrates the measured directivity index in dB versus frequency of both prototype arrays over the range of 125 Hz to 16 kHz.

8.3.1. Large-Driver Array

Figure 24 shows the directivity of the large-driver array. Directivity is maintained fairly well up to 5 kHz where it suddenly drops where the polar response widens. At higher frequencies, the

directivity rises due to the inherent high-frequency narrowing of the individual drivers.

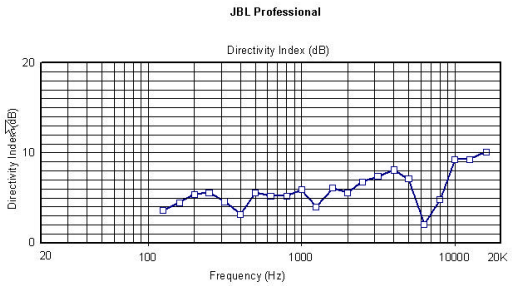

Fig. 24. Measured directivity index vs. frequency of the large-driver prototype array of Fig. 13.

8.3.2. Small-Driver Array

Figure 25 shows the directivity of the small-driver array. Directivity is well maintained over the range of 500 Hz to 16 kHz (5.5 ±1.5 dB).

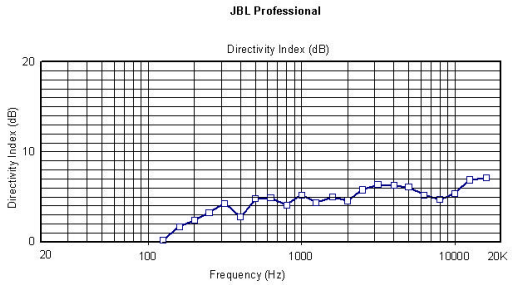

Fig. 25. Measured directivity index vs. frequency of the small-driver prototype array of Fig. 15.

8.4. Vertical Polars

This section illustrates the measured vertical polars of both prototype arrays.

8.4.1. Large-Driver Array

The measured vertical polars of the large-driver array are shown in Figs. 26 – 30 over the range of 200 Hz to 16 kHz. The vertical polars are quite consistent and well controlled up to 5 kHz, but widen uncontrollable at all higher frequencies. The array appears to work well up to the frequency where the spacing is equal to a wavelength. The 59 mm (2.32”) center-to-center spacing of the drivers is one wavelength at about 5.8 kHz.

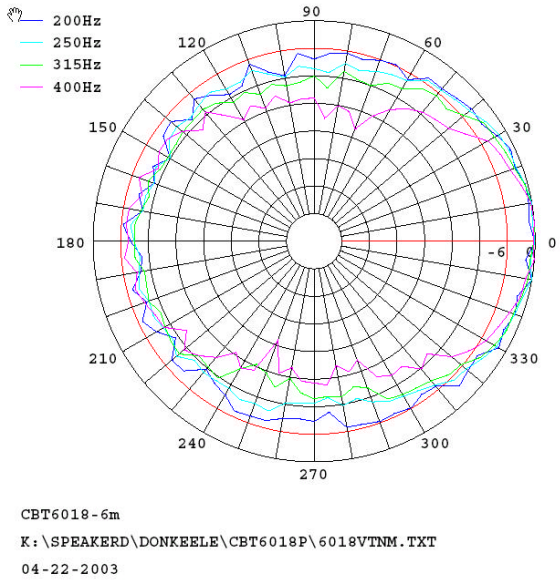

Fig. 26. Measured vertical polars at one-third-octave intervals over the range of 200 to 400 Hz for the large-driver array prototype of Fig. 13.

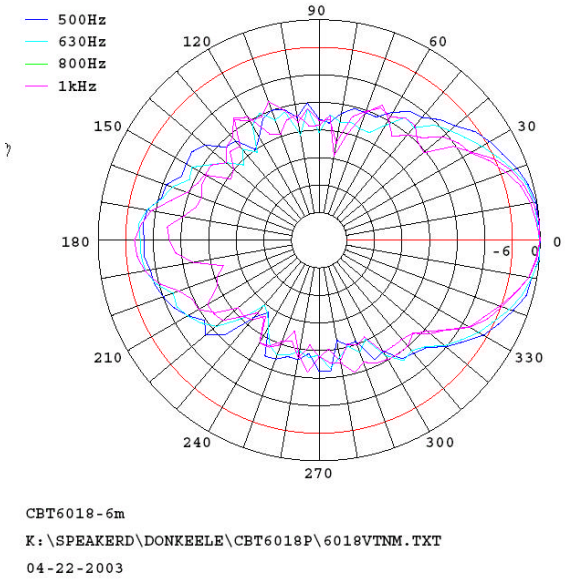

Fig. 27. Measured vertical polars at one-third-octave intervals over the range of 500 Hz to 1 kHz for the large-driver array prototype of Fig. 13.

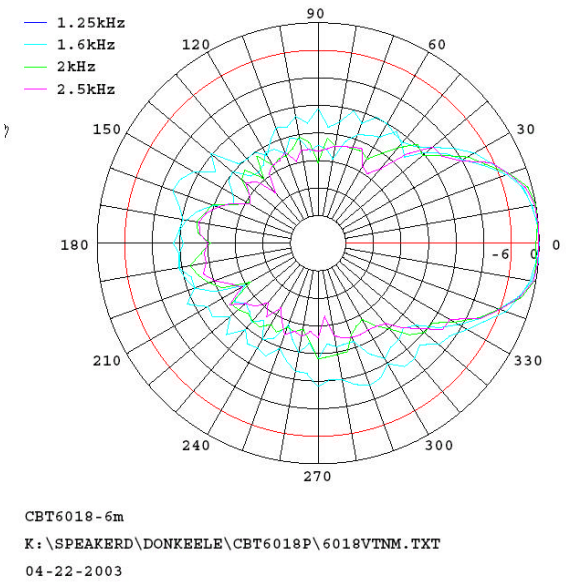

Fig. 28. Measured vertical polars at one-third-octave intervals over the range of 1.25 to 2.5 kHz for the large-driver array prototype of Fig. 13.

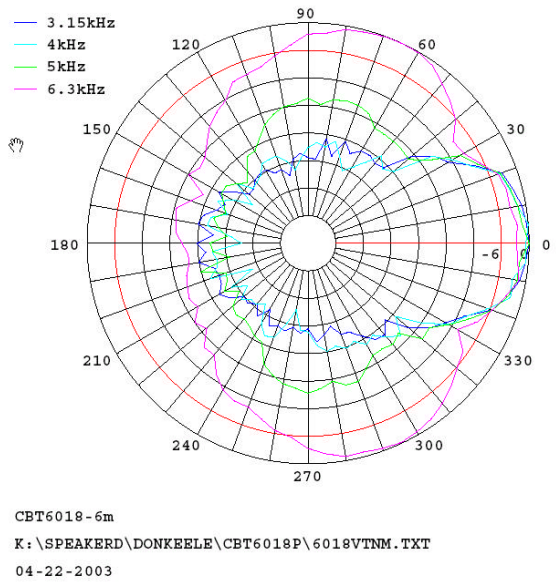

Fig. 29. Measured vertical polars at one-third-octave intervals over the range of 3.15 to 6.3 kHz for the large-driver array prototype of Fig. 13. Narrow coverage control is maintained only to 4 kHz. Note sudden widening at 6.3 kHz due to finite driver spacing becoming significant with respect to wavelength.

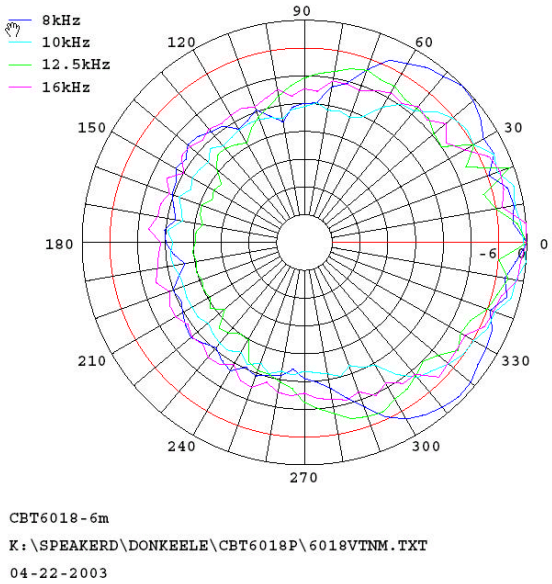

Fig. 30. Measured vertical polars at one-third-octave intervals over the range of 8 to 16 kHz for the large-driver array prototype of Fig. 13. Note very-wide coverage at all these frequencies due to incoherent summing of the driver's outputs due to spacing which is large with respect to wavelength. Some narrowing at the highest frequencies is evident due to the inherent coverage narrowing of the drivers themselves.

8.4.2. Small-Driver Array

The measured vertical polars of the small-driver array are shown in Figs. 31 – 35 over the range of 200 Hz to 16 kHz. The vertical polars are very consistent and well controlled all the way up to 16 kHz. The array appears to work well up to the frequency where the spacing is equal to a wavelength. The 21.2 mm (0.835") center-to-center spacing of the drivers is one wavelength at about 16.2 kHz.

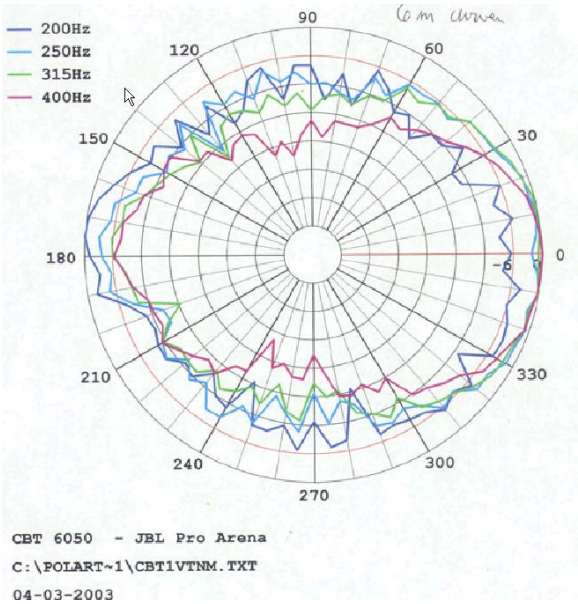

Fig. 31. Measured vertical polars at one-third-octave intervals over the range of 200 to 400 Hz for the small-driver array prototype of Fig. 15. Rapid variations in the polar pattern are due to signal-to-noise problems at low frequencies. The driver's output drops dramatically below 400 Hz.

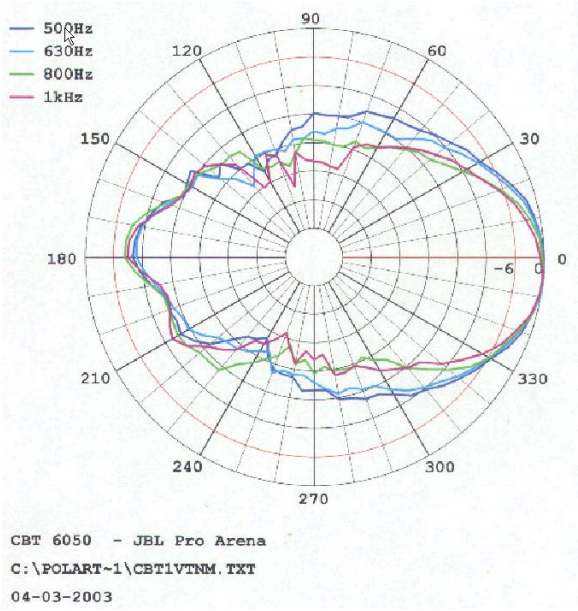

Fig. 32. Measured vertical polars at one-third-octave intervals over the range of 500 Hz to 1 kHz for the small-driver array prototype of Fig. 15.

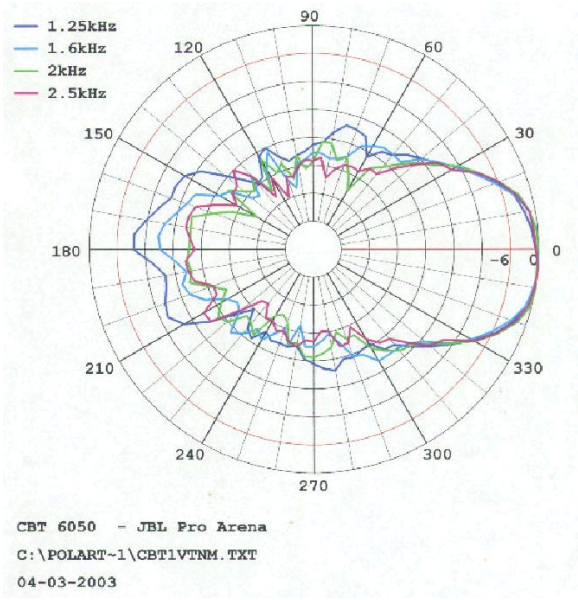

Fig. 33. Measured vertical polars at one-third-octave intervals over the range of 1.25 to 2.5 kHz for the small-driver array prototype of Fig. 15.

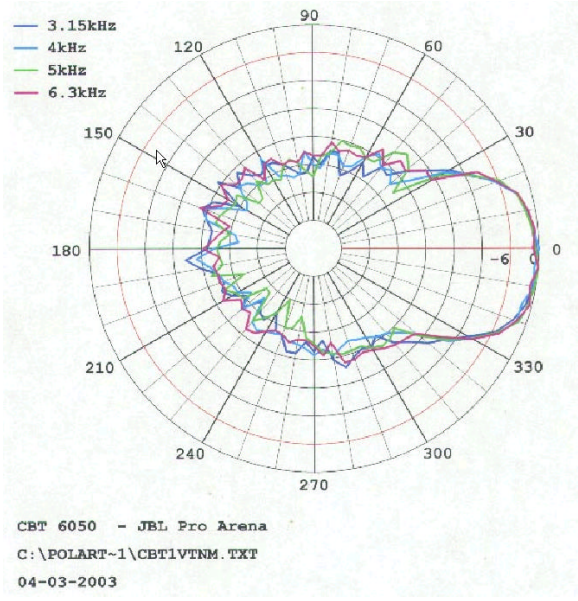

Fig. 34. Measured vertical polars at one-third-octave intervals over the range of 3.15 to 6.3 kHz for the small-driver array prototype of Fig. 15.

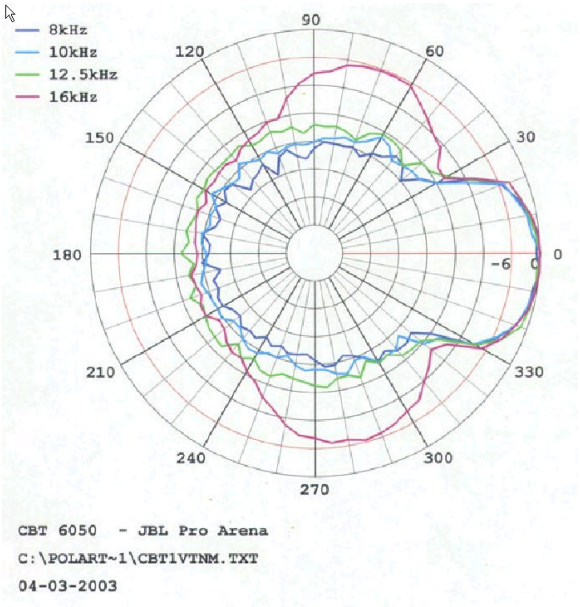

Fig. 35. Measured vertical polars at one-third-octave intervals over the range of 8 to 16 kHz for the small-driver array prototype of Fig. 15. Tight coverage control is maintained to 12.5 kHz. Note side lobes in the polar at 16 kHz due to finite driver spacing.

8.5. Full-Sphere Polar Balloons

This section illustrates some measured full-sphere polar directional balloons of both prototype arrays.

These polar balloons show the predicted 3D sound field of an array with a shape based on a deformed sphere whose radius in a particular direction is proportional to the array's radiated level (in dB) in that particular direction. The shape is scaled linearly such that a radius of 1 corresponds to 0 dB, a radius of 0.5 corresponds to -20 dB, and a radius of 0 (the center) corresponds to a level of –40 dB.

The balloons dB level is also color coded in a white – red – yellow – green – blue – violet – gray - black color scheme with white the high level and black the low level. The array's axis points down and to the left.

8.6. Large-Driver Array

Figures 36 and 37 show polar balloons of the large-driver prototype array at 2.5 and 8 kHz. Note the controlled and well-behaved balloon shape at 2.5 kHz. This balloon exhibits the characteristic eyeball shaped full-sphere sound pattern of the CBT curved-line array [5]. Note that the vertical coverage decreases as a function of the horizontal off-axis angle reaching a minimum at ±90° off axis.

At 8-kHz, the balloon exhibits severe vertical lobing because this frequency is above the control range of the array because the driver's spacing is significant with respect to wavelength.

8.6.1. 2.5 kHz Balloon

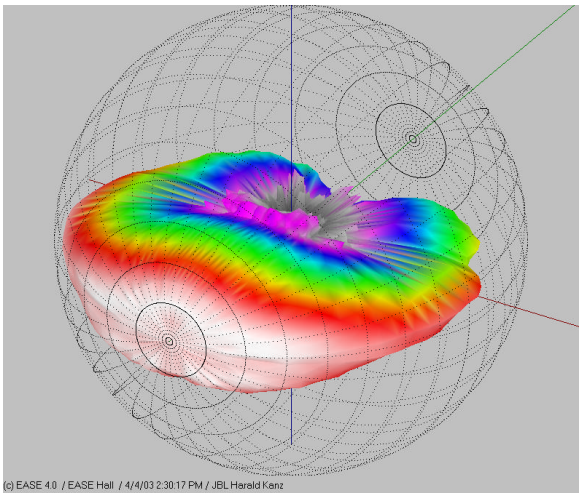

Fig. 36. Measured one-third-octave polar balloon at 2.5 kHz for the large-driver prototype array of Fig. 13. On axis points down and to the left. The array's coverage is very-well controlled at this frequency.

8.6.2. 8 kHz Balloon

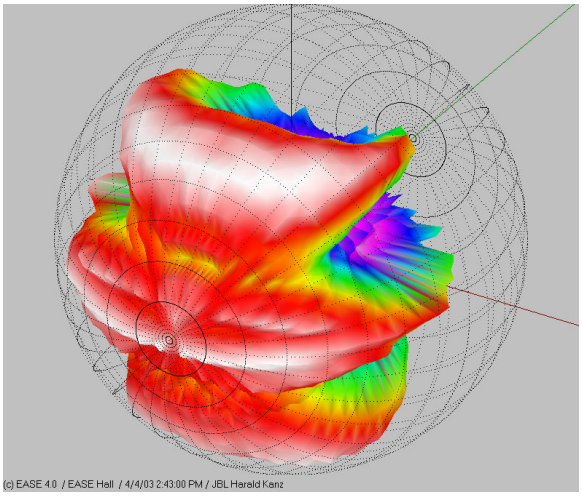

Fig. 37. Measured one-third-octave polar balloon at 8 kHz for the large-driver prototype array of Fig. 13. Note severe vertical lobing. At this frequency, the drivers are spaced to far apart for proper controlled vertical coverage.

8.7. Small-Driver Array

Figures 38 and 39 show polar balloons of the small-driver prototype array at 2.5 and 8 kHz. Both balloons are quite well-controlled because of the

small driver spacing. Balloons at 800 Hz and above, which are not shown, are also well behaved.

8.7.1. 2.5 kHz Balloon

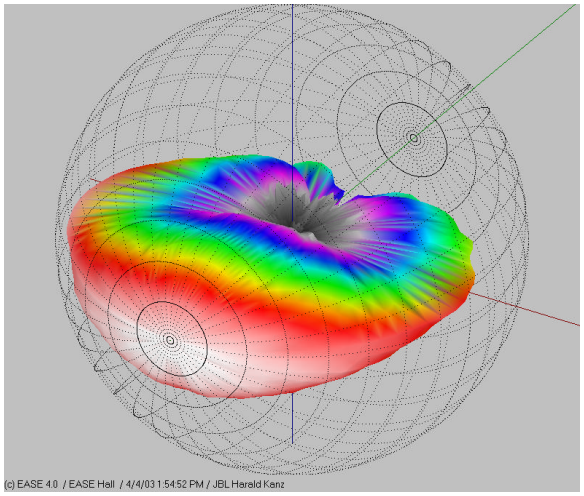

Fig. 38 Measured one-third-octave polar balloon at 2.5 kHz for the small-driver prototype array of Fig. 15. On axis points down and to the left. Balloon is well-behaved at this frequency.

8.7.2. 8 kHz Balloon

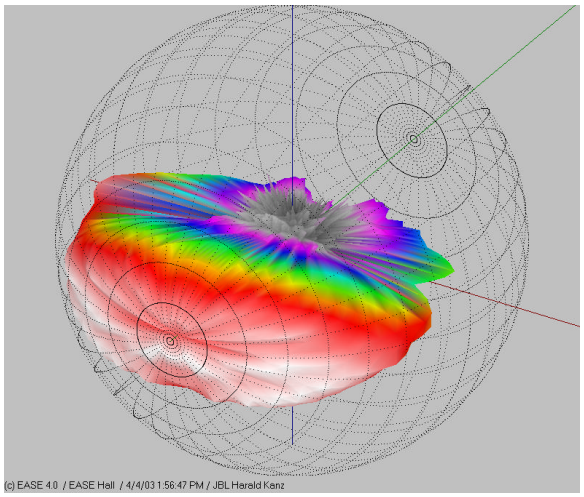

Fig. 39 Measured one-third-octave polar balloon at 8 kHz for the small-driver prototype array of Fig. 15. Proper narrow vertical coverage is maintained at this frequency.

9. CONCLUSIONS

This paper has shown that a properly functioning CBT curved-line array can be implemented with passive shading. The shading was implemented using a combination of parallel-series driver connections and resistor L-pad attenuators. It was shown that the CBT Legendre shading can be truncated and stepped without sacrificing the fine performance of the full-shaded CBT array. Best shading implementation resulted with a 3-dB step size that was truncated at the 12-dB-down level. This shading provided five discrete attenuation levels for the system's drivers.

Measurement results of two prototype arrays were very encouraging. Both arrays were measured using a full-sphere automated polar test system at 6m with rotation about the center of curvature of each array.

Measurements of the two prototype CBT curved-line arrays verified that a passively shaded array can provide extremely-uniform wideband coverage control with constant-beamwidth in both planes and solid constant-directivity characteristics.

The small-driver one-meter-high prototype CBT array, which used 50 each 17.8 mm (0.7") wide-band miniature transducers, provided an extremely uniform no-lobe vertical beamwidth coverage of about 46º (±4º) from 800 Hz to 16 kHz with a very-wide horizontal coverage of about 220º above 400 Hz. Vertical control was maintained down to 400 Hz where the beamwidth only rose to 65º. At lower frequencies the vertical and horizontal coverage was uncontrolled.

The large-driver one-meter-high prototype CBT array, which used 18 each 57mm (2.25") wide-band miniature transducers, also provided an extremely uniform no-lobe vertical beamwidth coverage of about 44º (±3º) but only from 800 Hz up to a much lower 5 kHz. Above 5 kHz the vertical beamwidth suddenly got very wide and then narrowed somewhat as the driver-to-driver spacing was significant with respect to wavelength. Horizontal coverage was also about 220º from 400 Hz to 8 kHz with narrowing at higher frequencies.

It was determined that operation to above 16 kHz does require the use of very-small closely-spaced wideband drivers. Because these very-small wideband drivers typically operate only down to 400 Hz or there about, full band operation down to 100 Hz would require at least a two-way system comprised of a combination of two side-by-side arrays, one using very-small drivers closely spaced, and the other using larger moderate-sized miniature drivers spaced farther apart.

10. REFERENCES

[1] P. H. Rogers, and A. L. Van Buren, "New Approach to a Constant Beamwidth Transducer," J. Acous. Soc. Am., vol. 64, no. 1, pp. 38-43 (1978 July).

[2] A. L. Van Buren, L. D. Luker, M. D. Jevnager, and A. C. Tims, "Experimental Constant Beamwidth Transducer," J. Acous. Soc. Am., vol. 73, no. 6, pp. 2200-2209 (1983 June).

[3] D. B. Keele, Jr., "The Application of Broadband Constant Beamwidth Transducer (CBT) Theory to Loudspeaker Arrays," 109th Convention of the Audio Engineering Society, Preprint 5216 (Sept. 2000).

[4] D. B. Keele, Jr., "Implementation of Straight-Line and Flat-Panel Constant Beamwidth Transducer (CBT) Loudspeaker Arrays Using Signal Delays," 113th Convention of the Audio Engineering Society, Preprint 5653 (Oct. 2002).

[5] D. B. Keele, Jr., "Full-Sphere Sound Field of Constant Beamwidth Transducer (CBT) Loudspeaker Line Arrays," J. Audio Eng. Soc., vol. 51, no. 7/8 (July/August 2003).

APPENDIX 1. REVIEW OF CBT THEORY

Quoting from Keele [3, Section 1]: "Rogers and Van Buren [1], and Buren et. al. [2] describe the theory and experiments of what they call broadband "constant beamwidth transducers" (CBT) for use as underwater projectors and receivers for sonar use. Here the transducer is in the form of a circular spherical cap of arbitrary half angle whose normal surface velocity (or pressure) is shaded with a Legendre function. The Legendre shading is independent of frequency. This transducer provides a broadband symmetrical directional coverage whose beam pattern and directivity is essentially independent of frequency over all frequencies above a certain cutoff frequency, and also change very little with distance from the source. The transducer can be designed to cover any arbitrary coverage angle with a constant beamwidth that extends over an operating bandwidth which is, in theory, virtually unlimited."

"Rogers and Van Buren [1] determined that if the radial velocity (or equivalently the surface pressure) on the surface of a rigid sphere of radius a conforms to

$$u(\theta) = \begin{cases} P_\nu(\cos\theta) & \text{for} \quad \theta \le \theta_0 \\ 0 & \text{for} \quad \theta > \theta_0 \end{cases} \qquad (1)$$

where

$u(\theta)$ = radial velocity distribution

θ = elevation angle in spherical coordinates,
($\theta = 0$ is center of circular spherical cap)

θ_0 = half angle of spherical cap

$P_\nu(x)$ = Legendre function of order ν ($\nu > 0$) of argument x,

then an approximation to the farfield pressure pattern, above a cutoff frequency which depends on the size of the sphere and the wavelength, will be

$$p(\theta) = \begin{cases} P_\nu(\cos\theta) & \text{for} \quad \theta \le \theta_0 \\ 0 & \text{for} \quad \theta > \theta_0 \end{cases} \qquad (2)$$

where

$p(\theta)$ = radial pressure distribution.

"This surprising result shows that the farfield sound pressure distribution is essentially equal to the pressure distribution on the surface of the sphere. Rogers and Van Buren also point out that because the surface pressure and velocity are nearly zero over the inactive part of the outside surface of the sphere, the part of the rigid spherical shell outside the spherical cap region can be removed without significantly changing the acoustic radiation. This means that the ideal constant beamwidth behavior of the spherical cap is retained even though the rest of the sphere is missing!"

"The Legendre function $P_\nu(\cos\theta)$ is equal to one at $\theta = 0$ and has its first zero at angle $\theta = \theta_0$, the half angle of the spherical cap. The Legendre function order (ν) is chosen so that its first zero occurs at the half angle of the spherical cap. Note that ν is normally greater than one, and not necessarily an integer."

"Rogers and Van Buren also point out that the constant beamwidth behaviour of a rigid spherical cap also applies as well to an acoustically transparent spherical shell. However the acoustic radiation is bidirectional, generating the same beam pattern front and rear."

"To sum up the advantages of the CBT I quote from [1]:

"We enumerate the expected properties of the CBT above cutoff:

(1) Essentially constant beam pattern.
(2) Very low sidelobes.
(3) The surface distribution as well as the pressure distribution at all distances out to the farfield is approximately equal to the surface distribution. Thus in a sense, there is no nearfield.
(4) Since both the surface velocity and surface pressure have the same dependence on θ, the local specific acoustic impedance is independent of θ (and equal to $\rho_0 c$). Thus the entire transducer is uniformly loaded.""

Keele [3] extends the CBT theory to loudspeaker arrays and provides a simplified four-term series approximation to the Legendre shading of Eq. (1) which is acceptable over all useful Legendre orders:

$$U(x) \approx \begin{cases} 1 + 0.066x - 1.8x^2 + 0.743x^3 & \text{for} \quad x \le 1 \\ 0 \quad \text{for} \quad x > 1 \end{cases} \quad (3)$$

where

x = normalized angle $\left(\dfrac{\theta}{\theta_0} \right)$

Note that this function is exactly 1 at $x = 0$ and 0 at $x = 1$ (where $\theta = \theta_0$ the half cap angle). All the following simulations use eq. (3) as a substitute for the Legendre function of Eq. (1).

As pointed out in [3], the coverage angle (6-dB-down beamwidth) of the CBT array is approximately 64% of the cap angle or circular-arc angle.

Keele [3, 4] extended the CBT theory to circular-arc line arrays. Here the array is a circular-arc or wedge, usually oriented with its long axis vertical. This current paper presents methods to practically implement CBT circular-arc line arrays .

APPENDIX 2. ARRAY SIMULATOR

The point-source array simulator program used in [3 - 5] was used to predict the directional characteristics of the arrays in this paper. This program calculates the pressure distribution at a specific distance (all simulations here are done at a far-field distance of 250m) for a 3-D array of point sources of arbitrary magnitude and phase.

Polar rotations were all done around the center of the coordinate system. Note that all the conventional curved CBT arrays were offset so that their centers of curvature coincided with the center of the coordinate system.

Program outputs include:

1. Source configuration views as seen from front, top, and sides.

2. Horizontal and vertical beamwidth (-6dB) vs. frequency plots at each one-third-octave center from 20 Hz to 16 kHz.

3. Directivity index and Q vs. frequency plots at each one-third-octave center from 20 Hz to 16 kHz.

4. On-axis frequency response (loss) plot vs. frequency (compared to all sources on and in-phase at the pressure sampling point). This plot indicates how much on-axis attenuation the array imposes as compared to the situation where all the sources add in phase at the sampling point.

5. Complete set of ±60º horizontal x ±60º vertical normalized SPL footprint plots at all one-third octaves over the frequency range of 20 Hz to 16 kHz. In each footprint plot, the pressure in dB is normalized to the maximum in the stated angular range and is shown as a grey-scale density plot (high pressure in white (0 dB) and low in black (-20 dB)).

APPENDIX 3. VARIATION OF CBT SHADING (Simulated using 1-m-high, 62.5°-wedge-angle curved-line CBT array.)

TABLE 1: Variation of Stepped CBT Legendre Shading

DESCRIPTION	CONTINUOUS SHADING	3-dB STEPPED SHADING	6-dB STEPPED SHADING	9-dB STEPPED SHADING	SINGLE STEP (No Shading)
SHADING	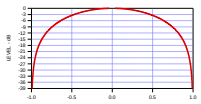	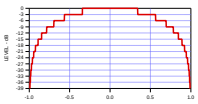	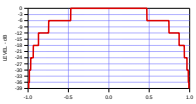	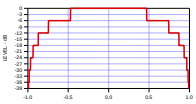	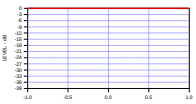
BEAMWIDTH	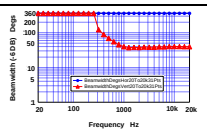	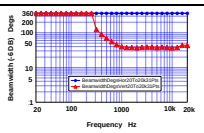	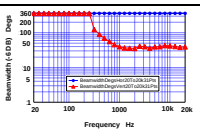	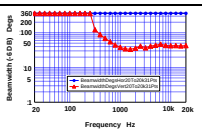	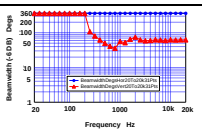
DIRECTIVITY	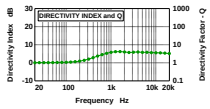	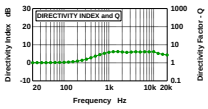	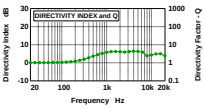	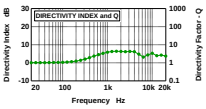	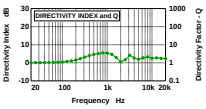
VERTICAL POLARS 800 Hz	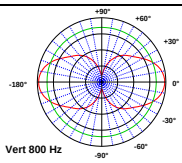	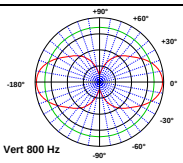	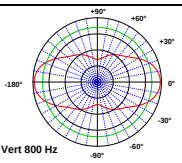	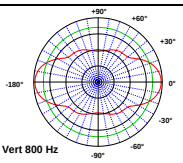	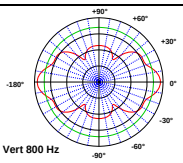
VERTICAL POLARS 1.6 kHz	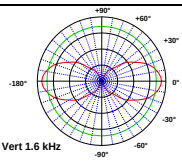	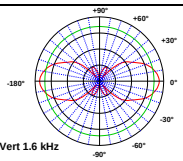	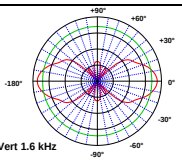	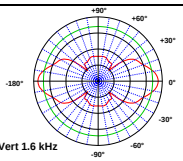	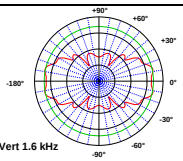
VERTICAL POLARS 3.15 kHz	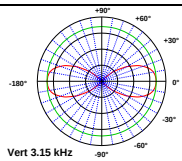	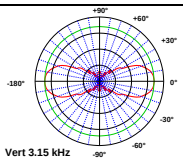	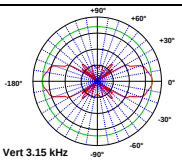	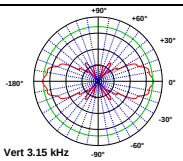	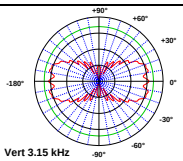
VERTICAL POLARS 6.3 kHz	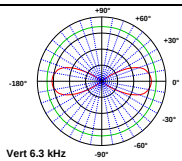	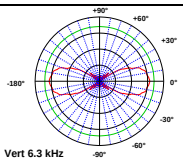	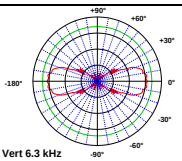	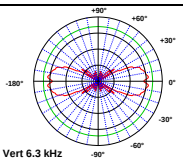	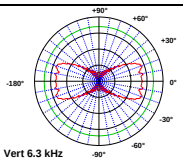
VERTICAL POLARS 12.5 kHz	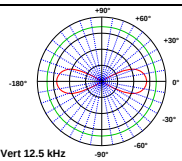	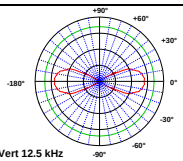	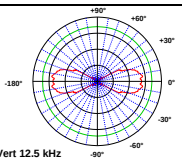	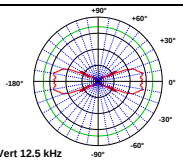	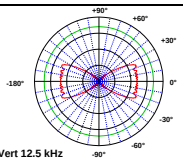

TABLE 2: Variation of Truncated CBT Legendre Shading

DESCRIPTION	TRUNCATED AT –18 db	TRUNCATED AT –15 db	TRUNCATED AT –12 db	TRUNCATED AT –9 db	TRUNCATED AT –6 db
SHADING	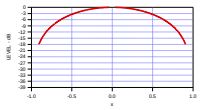	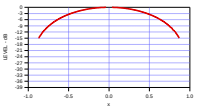	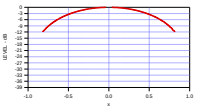	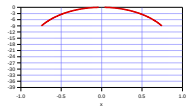	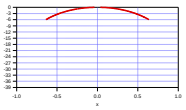
BEAMWIDTH	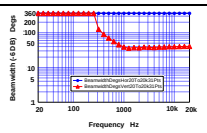	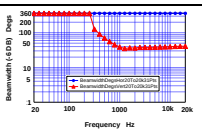	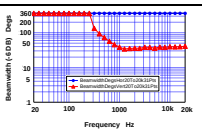	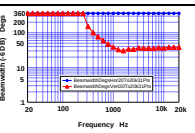	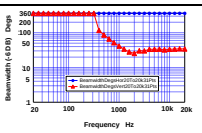
DIRECTIVITY	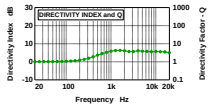	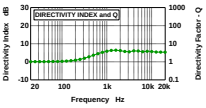	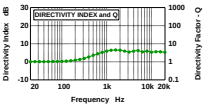	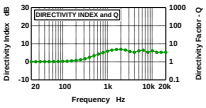	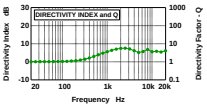
VERTICAL POLARS 800 Hz	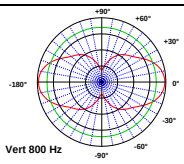	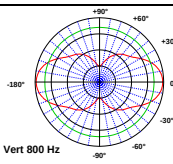	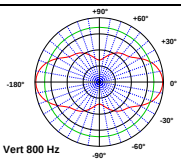	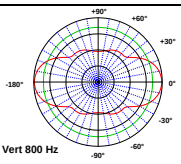	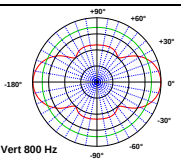
VERTICAL POLARS 1.6 kHz	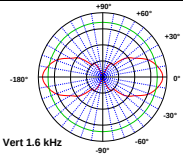	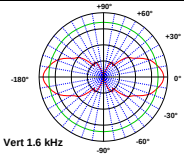	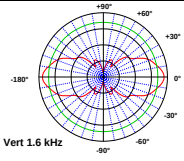	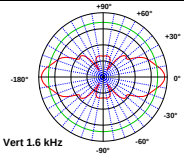	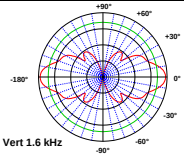
VERTICAL POLARS 3.15 kHz	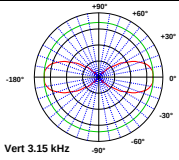	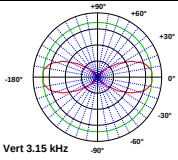	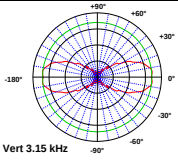	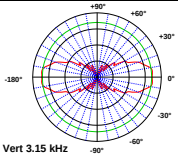	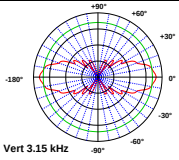
VERTICAL POLARS 6.3 kHz	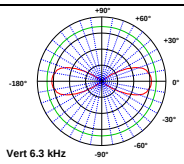	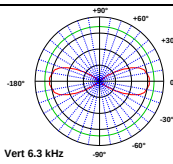	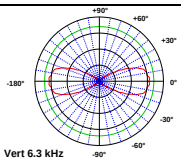	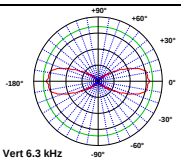	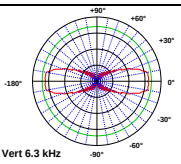
VERTICAL POLARS 12.5 kHz